AD-A133 258 APPLICATION OF TWO-DIMENSIONAL DISCRETE-ORDINATES METHODS TO MULTIPLE SCA..(U) ARMY ARMAMENT RESEARCH AND DEVELOPMENT COMMAND ABERDEEN PROVI.. A ZARDECKI ET AL. 1/1

UNCLASSIFIED JUN 83 ARCSL-TR-83022 F/G 12/1 NL

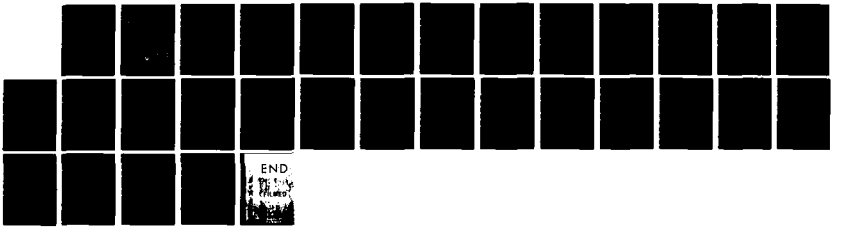

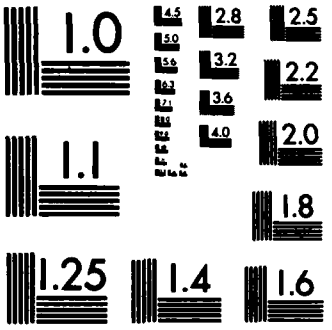

(12)

AD

CHEMICAL SYSTEMS LABORATORY

US Army Armament Research and Development Command
Aberdeen Proving Ground, Maryland 21010

TECHNICAL REPORT

ARCSL-TR-83022

APPLICATION OF TWO-DIMENSIONAL DISCRETE-ORDINATES METHOD TO MULTIPLE SCATTERING OF LASER RADIATION

by

A Zardecki
S. A. W. Gerstl

Los Alamos National Laboratory

J. F. Embury

Physics Branch
Research Division

June 1983

Approved for public release; distribution unlimited.

Disclaimer

The findings in this report are not to be construed as an official Department of the Army position unless so designated by other authorized documents.

Disposition

Destroy this report when it is no longer needed. Do not return it to the originator.

UNCLASSIFIED

SECURITY CLASSIFICATION OF THIS PAGE *(When Data Entered)*

REPORT DOCUMENTATION PAGE	READ INSTRUCTIONS BEFORE COMPLETING FORM
1. REPORT NUMBER: ARCSL-TR-83022 — 2. GOVT ACCESSION NO.: AD-A133258	3. RECIPIENT'S CATALOG NUMBER
4. TITLE *(and Subtitle)*: APPLICATION OF TWO-DIMENSIONAL DISCRETE-ORDINATES METHOD TO MULTIPLE SCATTERING OF LASER RADIATION	5. TYPE OF REPORT & PERIOD COVERED: December 6, 1982-February 17, 1983
	6. PERFORMING ORG. REPORT NUMBER
7. AUTHOR(s): A Zardecki, S. A. W. Gerstl, J. F. Embury	8. CONTRACT OR GRANT NUMBER(s)
9. PERFORMING ORGANIZATION NAME AND ADDRESS: Commander, Chemical Systems Laboratory, ATTN: DRDAR-CLB-PS, Aberdeen Proving Ground, Maryland 21010	10. PROGRAM ELEMENT, PROJECT, TASK AREA & WORK UNIT NUMBERS: 1L162622A552
11. CONTROLLING OFFICE NAME AND ADDRESS: Commander, Chemical Systems Laboratory, ATTN: DRDAR-CLJ-IR, Aberdeen Proving Ground, Maryland 21010	12. REPORT DATE: June 1983
	13. NUMBER OF PAGES: 34
14. MONITORING AGENCY NAME & ADDRESS*(if different from Controlling Office)*	15. SECURITY CLASS. *(of this report)*: UNCLASSIFIED
	15a. DECLASSIFICATION/DOWNGRADING SCHEDULE: NA

16. DISTRIBUTION STATEMENT *(of this Report)*

Approved for public release; distribution unlimited.

17. DISTRIBUTION STATEMENT *(of the abstract entered in Block 20, if different from Report)*

18. SUPPLEMENTARY NOTES

19. KEY WORDS *(Continue on reverse side if necessary and identify by block number)*

Code TWOTRAN	Delta-M approximation	CDC-7600 computer
Laser multiple scattering	Linear Boltzmann equation	Cray-1 computer
Discrete ordinates 2D	Radiance distribution function	Code THREETAN
Lambert-Beer law	Standard numerical algorithms	Computer time
X-y and r-z geometry	Phase space points	(Continued on reverse side)

20. ABSTRACT *(Continue on reverse side if necessary and identify by block number)*

The discrete-ordinates finite element radiation transport code TWOTRAN is applied to describe the multiple scattering of a laser beam from a reflecting target. For a model scenario involving a 99% relative humidity rural aerosol, we compute the average intensity of the scattered radiation and correction factors to the Lambert-Beer law arising from multiple scattering. As our results indicate, two-dimensional x-y and r-z geometry modeling can reliably describe a realistic three-dimensional scenario.
(Continued on reverse side)

DD FORM 1 JAN 73 1473 EDITION OF 1 NOV 65 IS OBSOLETE

UNCLASSIFIED

SECURITY CLASSIFICATION OF THIS PAGE *(When Data Entered)*

19. KEYWORDS (continued)

General anisotropic scattering	Pointwise convergence	Expansion coefficients
Collimated Gaussian beam	Volume extinction coefficient	Extinction coefficient
Ground reflectivity	Koschmeider formula	Scattering phase function
Dirac delta function	Eddington approximation	Legendre polynomials
Number 2M-1		AGAUSX code

20. ABSTRACT (continued)

Specific results are presented for the two visual ranges of 1.52 and 0.76 km which show that for sufficiently high aerosol concentrations (e.g., equivalent to V = 0.76 km) the target signature in a distant detector becomes dominated by multiply scattered radiation from interactions of the laser light with the aerosol environment. The merits of the scaling group and the delta M approximation for the transfer equation are also explored.

PREFACE

Funds for the testing and recording of results presented in this report were supplied from Project 1L162622A552, Application of 2D Discrete-Ordinates Method to Multiple Scattering of Laser Radiation. The work reported was carried out from 6 December 1982 to 17 February 1983. It was authorized by the same project and test area above.

The use of trade names in this report does not constitute an official endorsement or approval of the use of such commercial hardware or software. This report may not be cited for purposes of advertisement.

This report has been approved for release to the public.

BLANK

CONTENTS

Blank

APPLICATION OF TWO-DIMENSIONAL DISCRETE-ORDINATES METHOD TO MULTIPLE SCATTERING OF LASER RADIATION

1. INTRODUCTION

Light propagation through an optically thick particulate medium is basically a multiple-scattering problem in which rays or photons traverse a medium of scatterers and undergo many scattering events before escaping. A natural framework to deal with this type of problem is provided by the theory of radiative transfer. The linear Boltzmann equation - in the context of radiative energy also termed the "equation of transfer" - governs the radiation field in a medium that absorbs, emits, and scatters radiation.[1]

The complexity of the equation of transfer forces one to implement numerical methods of solution. Such methods seek to introduce approximations that convert the integro-differential form of the equation of transfer into a system of algebraic equations that is amenable to solution by a digital computer.[2] The most direct procedure is the discrete-ordinates approach in which the radiance distribution function $I(\vec{r},\vec{\Omega},\lambda)$ is replaced by a discrete set of values at a discrete set of phase space points $(\vec{r}_i,\vec{\Omega}_j,\lambda_k)$. The derivatives and integrals appearing in the equation of transfer must also be replaced by a corresponding discrete representation using finite difference and numerical integration schemes. In this way one arrives at a set of algebraic equations that can be solved by using standard numerical algorithms on a digital computer.

Unfortunately, such a calculation becomes an immense undertaking if only a "brute force" discretization of the equation of transfer is employed. For example, a typical mesh size of 100 by 100 by 100 space points, 10 wavelength groups, and 10 discrete angles would yield an extremely large set of simultaneous algebraic equations involving at least 10^8 discrete phase space points, which is a rather formidable task even on the CDC-7600 or Cray-1 computers.

The discrete-ordinates method is discussed in detail in references 1-5. In the context of neutron transport theory, a comprehensive treatment is contained in the monograph of Bell and Glasstone.[6] Modern neutron transport methods have only recently been applied to atmospheric radiative transfer problems by Gerstl.[7] Following reference 5, we summarize the main features of the method:

(a) The solution of the transfer equation may be derived explicitly and therefore the intensity and flux computations do not only depend on the total optical depth of aerosol layers.

(b) The method yields the radiation field at all spatial locations as well as the reflection and transmission without additional computational effort.

(c) The computer time required to calculate intensity and flux is relatively small as compared with other techniques.

For two- and three-dimensional geometries, the solution of the discrete-ordinates equations becomes increasingly complex. Extensions from two to three dimensions result in severe computational problems because of the sheer size of the system of equations rather than any basic complications in numerical solution algorithms from the added dimension. A discrete-ordinates code THREETRAN[8] which is capable of treating three-dimensional geometry, exists only in an experimental version.

When looking for rigorous solutions to the problem of light scattering and propagation in dense aerosols, it thus becomes imperative to explore the usefulness and the range of applicability of the existing two-dimensional transport codes. We note that radiative transfer in two dimensions has earlier been studied by Fowler[9] and Fowler and Sung.[10] The purpose of this paper is to apply the two-dimensional code TWOTRAN[11] to the description of a laser beam scattered (reflected) from a fixed target. This is obviously relevant to the evaluation of the effectiveness of electro-optical systems under aerosol-loaded and adverse weather conditions. After summarizing the main features of the TWOTRAN code and the solution algorithm in section 2, we make use in section 3 of the advantages of the delta M method.[12] In section 4, we describe our model scenario where a collimated laser beam propagating in a homogeneous rural aerosol is subsequently scattered from an isotropic target. The average intensity and Beer/Lambert correction factor are introduced in section 5. They allow us to make a comparative study of results in the rectangular (x-y) and cylindrical (r-z) geometries, which is contained in section 6. Section 7 is devoted to the discussion of the results obtained, and conclusions outlining future lines of research.

2. SOLUTION ALGORITHM

For calculations reported here, the general-purpose code TWOTRAN-II has been adapted to radiative transfer calculations of a laser beam in a realistic aerosol medium.

TWOTRAN-II is a general purpose FORTRAN code that solves the two-dimensional multigroup transport equation in (x,y), (r,θ), and (r,z) geometries. Both regular and adjoint, inhomogeneous and homogeneous problems subject to vacuum, reflective, periodic, white or input-specified boundary flux conditions are solved. General anisotropic scattering is allowed and anisotropic inhomogeneous sources are permitted.

The discrete ordinates approximation for the angular variable is used in finite difference form which is solved with the central (diamond) difference approximation. Negative fluxes are eliminated by a local set-to-zero and correct algorithm. Standard inner and outer iterative cycles are accelerated by coarse mesh which may be independent of the material mesh. Our computations with TWOTRAN performed with a pointwise convergence criterion of 2×10^{-2} using 144 discrete directions (S_{16}) and 42 by 42 mesh point required the running time of 1.2-1.5 min on the CDC-7600 machine.

In the absence of volumetric sources, the equation of transfer to be solved is

$$\underline{\Omega}\cdot\nabla I(\underline{r},\underline{\Omega}) + \sigma_t(\underline{r})I(\underline{r},\underline{\Omega}) = \int \sigma_s(\underline{r},\hat{\mu})I(\underline{r},\underline{\Omega}')d\Omega' \tag{1}$$

where

σ_t is the volume extinction coefficient and $I(\underline{r}, \underline{\Omega})$ is the radiance distribution function. In nuclear radiation transport terminology, $\sigma_s(r, \hat{\mu})$ is the differential-scattering-transfer cross section, where $\hat{\mu}$ is the cosine of the angle between the directions $\underline{\Omega}'$ and $\underline{\Omega}$ of the incoming and outgoing pencils of radiation. In terms of $\sigma_s(r,\hat{\mu})$, the scattering phase function, $P(\underline{r},\hat{\mu})$, is given by

$$P(\underline{r},\hat{\mu}) = \sigma_s(\underline{r},\hat{\mu})/\sigma_s^0(\underline{r}) \tag{2}$$

with the normalizaton

$$\int P(\underline{r},\hat{\mu})d\hat{\mu} = 1 \tag{3}$$

$$\int \sigma_s(\underline{r},\hat{\mu})d\hat{\mu} = \sigma_s^0(\underline{r}) \tag{4}$$

where

$\sigma_s(\underline{r})$ is the volume scattering coefficient at location $\underline{r}$.

In two-dimensional x-y and r-z geometries, the TWOTRAN code requires the sets of spatial meshes (x_k, y_ℓ) or (r_k, z_ℓ) and discrete directions $\{\Omega_m\}$. We always choose the beam axis in the y or z directions, in x-y and r-z geometries, respectively. As the set of discrete directions $\{\Omega_m\}$ is determined by the choice of a Gaussian quadrature, there will be usually no direction available along the y or z axes. It is therefore convenient to divide the total radiance into two parts, the reduced I_{ri} and the diffuse radiance I_d. The reduced radiance satisfies equation (1) with the right-hand side set equal to zero. In the x-y geometry, for example, it is

$$I_{ri}(\underline{\Omega},\underline{r}) = I(\underline{\Omega}, x - y\Omega_x/\Omega_y, 0)\ \exp\left[-\frac{1}{\Omega_y}\int_0^y \sigma_t(x - y'\Omega_x/\Omega_y, y')dy'\right] \tag{5}$$

where

Ω_x and Ω_y are the components of the vector $\underline{\Omega}$ in the plane x-y.

The diffuse radiance satisfies the equation

$$\underline{\Omega}\cdot\nabla I_d(\underline{r},\underline{\Omega}) + \sigma_t(\underline{r})I_d(\underline{r},\underline{\Omega}) = \int \sigma_s(\underline{r},\hat{\mu})I_d(\underline{r},\underline{\Omega}')d\underline{\Omega}' + Q(\underline{r},\underline{\Omega}) \tag{6}$$

where Q is the source function

$$Q(\underline{r},\underline{\Omega}) = \int \sigma_s(\underline{r},\hat{\mu})I_{ri}(\underline{r},\underline{\Omega}')d\Omega' \tag{7}$$

generated by the reduced radiance.

In order to obtain the solution for the diffuse radiance from the TWOTRAN program, both σ_s and Q should be represented by finite Legendre polynomial expansions. The function $\sigma_s(\underline{r},\hat{\mu})$ is written as

$$\sigma_s(\underline{r},\hat{\mu}) = \sum_{i=0}^{L} \frac{2\ell + 1}{4\pi}\sigma_s^\ell(\underline{r})P_\ell(\hat{\mu}) \tag{8}$$

where the expansion coefficients σ_s^ℓ are assumed to be known. To write down an expansion for the source function Q, we take the case of rectangular x-y geometry as an example. For a collimated laser beam with the spatial shape described by a function F(x) at y = 0

$$I(x,y=0,\underline{\Omega}) = F(x)\delta(\underline{\Omega} - \hat{y}) \tag{9}$$

by virtue of equation (5) the reduced radiance becomes

$$I_{ri}(\underline{\Omega},\underline{r}) = F(x)\delta(\underline{\Omega} - \hat{y})\exp\left[-\int_0^y \sigma_t(x,y')dy'\right] \tag{10}$$

Equation (7) now yields

$$Q(\underline{r},\underline{\Omega}) = F(x)\sigma_s(\underline{r},\underline{\Omega}\cdot\hat{y})\exp\left[-\int_0^y \sigma_t(x,y')dy'\right] \tag{11}$$

As is evident by inspection of equations (8) and (11), the expansion of the source function involves the series expansion of equation (11) with the Legendre polynomials $P_i(\hat{\Omega}\hat{\Omega})$ taken at the argument $P_\ell(\Omega_y)$. For strongly asymmetric phase functions, the computational difficulties arise because such phase functions cannot be represented by polynomials of low degree. A way out of the predicament is the delta M method, which we will now discuss in the context of the TWOTRAN transport code.

3. THE DELTA M METHOD FOR THE TWOTRAN CODE

The delta M method, which relies essentially on matching the first 2M phase function moments and using a Dirac delta function representation of forward scattering, is an extension of the δ - Eddington approximation.[13] The method has recently been discussed in connection with the scaling group of the radiative transfer equation.[14] In order to adapt the delta M method for our purposes, we note that the only physical quantities required to run the TWOTRAN code are the expansion coefficients σ_s^{ℓ} in equation (8) and the extinction coefficient σ_t at each mesh side. When the phase function is approximated by a Dirac delta function forward peak and a (2M - 1)-term expansion, the function σ_s in equation (8) becomes

$$^{*}\sigma_s(\underline{r},\hat{\mu}) = \sum_{\ell=0}^{2M-1} \frac{2\ell + 1}{4\pi} \, ^{*}\sigma_s^{\ell}(\underline{r}) P_i(\hat{\mu}) \tag{12}$$

where for highly asymmetric phase functions the number 2M-1 will be much smaller than L. The condition that the first (2M-1)-phase-function moments be matched exactly leads to

$$^{*}\sigma_s^{\ell}(\underline{r}) = \sigma_s^{\ell}(\underline{r}) - f \tag{13}$$

with

$$f = \sigma_s^{2M}(\underline{r}) \tag{14}$$

Since the extinction coefficient transforms as

$$^{*}\sigma_t = \sigma_t - f\sigma_s^0 \quad , \tag{15}$$

the new equation of transfer for the transformed radiance I* becomes

$$\underline{\Omega}\cdot\nabla I^{*} + {}^{*}\sigma_t I^{*} = \int {}^{*}\sigma_s(\underline{r},\hat{\mu}) I^{*}(\underline{r},\underline{\Omega}')d\Omega' \tag{16}$$

Thus, by comparing equation (16) with equation (1), we see that the delta M method does not change the functional form of the transfer equation.

Actually, as explained in section 2, we solve the equation of transfer for the diffuse radiance. This is obtained from equation (6), in which the σ_s and σ_t have been transformed according to equations (12) and (15). The reduced part of the radiance is still given by a simple analytic expression, obtained by combining equations (5) and (15):

$$I_{ri}^{*} = I_{ri} \exp\left[\frac{1}{\Omega_y} \int_0^y (f\sigma_x^0)(x - y'\Omega_x/\Omega_y, y')dy' \right] \tag{17}$$

For a homogeneous medium, with the collimated laser beam propagating along the y axis, equation (17) simpifies to

$$I_{ri}^{*} = I_{ri} \exp(f\sigma_s^0 y) \tag{18}$$

Therefore, from the approximate equality

$$I_{ri} + I_d = I_{ri}^{*} + I_d^{*} \tag{19}$$

$$C \equiv \frac{I_d}{I_{ri}} = \exp(f\sigma_s^0 y) - 1 + \frac{I_d^*}{I_{ri}} \tag{20}$$

Equation (20) enables one to evaluate the multiple-scattering corrections to the exponential decay expressed by the Beer–Lambert law.

4. MODEL SCENARIO

In this section we describe the results pertaining to a simple scenario in which the scattering medium is formed by a homogeneous distribution of 99% relative humidity rural aerosol. The rural model, as developed by the Air Force Geophysics Laboratory,[15] is intended to represent the aerosol conditions one finds in continental areas which are not directly influenced by industrial aerosol sources. The optical characteristics of the medium are generated with the aid of the AGAUSX code, as described in references 16 and 17. Figure A-1 (appendix A) shows relative locations of the laser source and the isotropically reflecting target in the x-y (r–z) plane. The x (r) axis, named also "height", is chosen perpendicular to the surface of the earth, while the y (z) axis, named "distance" is taken along the axis of symmetry of the laser beam. In r–z geometry, the medium has an azimuthal (rotational) symmetry around the z axis. The symmetry condition in x-y geometry may be illustrated by imagining that the medium is infinite in extent in the direction perpendicular to the x-y plane. Both the x (r) and y (z) directions are divided into six coarse mesh cells whose boundaries are given by x (r) = 0.0, 0.002, 0.010, 0.050, 0.8, 1.0, 2.5 km, and y (z) = 0.0, 3.0, 3.8, 4.0, 4.006, 4.106 and 4.4 km. In addition, each coarse mesh cell is subdivided into fine mesh cells of equal width. In the x (r) direction, the sequence 2, 8, 10, 10, 2, 10 specifies the number of fine meshes per coarse mesh. The corresponding numbers in the y (z) directions are 20, 8, 5, 2, 4 and 3. Thus the x-y (r-z) plane has been covered by 42 x 42 fine mesh cells with unequal sides. In x-y geometry, the coordinates of the laser source are x_o = 1.5 m and y_o = 3.0 km. The source emits a Gaussian collimated beam with the radiance distribution for $y = y_o$ given by the formula

$$I(x,y_o,\vec{\Omega}) = F/(\pi^{1/2}w)\exp[-(x-x_o)^2/w^2]\delta(\vec{\Omega}-\vec{y}) \quad , \tag{21}$$

where F is the total energy of the beam, and δ denotes the Dirac delta function. In realistic situations, one usually deals with a pulse source. Typically, the emitted pulses are of 1 MW power and 20 nsec duration. We thus set F = 2 x 10^{-2} J per pulse and take w = 0.5 m. As the distance between the source and the target is equal to 1 km, a point source having the divergence of 1 mrad would produce a spot of 1 m in diameter at the target's location. The collimated Gaussian beam with half width w = 0.5 can therefore be viewed as a beam equivalent to that produced by a divergent point source, at least as far as the target illumination is concerned. The target, with assumed reflectivity r_t = 0.5, reradiates the incident beam isotropically generating a diffuse radiation field in the x-y plane. The ground reflectivity (surface albedo) for x = 0 is assumed to be r_g = 0.1. In r-z geometry, the radiance distribution function in the plane $z = z_o$ is given as

$$I(r,z_o,\vec{\Omega}) = \frac{F}{\pi w^2}\exp(-r^2/w^2)\delta(\vec{\Omega} - \vec{z}) \tag{22}$$

Equation (22) implies that the beam axis coincides with the z-axis. As before we take z_o = 3 km and suppress the ground reflectivity r_g. For rectangular x-y geometry, as the beam is parallel to the ground surface x = 0, the exact value of r_g has only a negligible effect on the results of our calculations.

We choose the concentration of the aerosol particles to be described by the number density of 50,000 particles per cm^3. This corresponds to the extinction coefficient $\sigma = 1.32$ km^{-1} at the wavelength $\lambda = 1.06\,\mu m$. For $\lambda = 0.55\,\mu m$ the extinction coefficient is 2.57 km^{-1}. The meterological (visual) range V, as defined by the Koschmieder formula

$$V = \frac{3.912}{\sigma(\lambda=0.55\ \mu m)} \quad , \tag{23}$$

is then V = 1.52 km. As the number density increases to 100,000 particles per cm^3, the extinction coefficient becomes $\sigma = 2.64$ km^{-1} and the meteorological range decreases to V = 0.76 km. The optical depths at $\lambda = 1.06\,\mu m$ for the distance between laser and the target (1 km) in the two cases considered are 1.32 (for V = 1.52 km) and 2.64 (for V = 0.76 km).

5. AVERAGE INTENSITY AND BEER-LAMBERT CORRECTION FACTOR

The knowlege of the radiance distribution function $I(\vec{r},\vec{\Omega})$ allows us to introduce the average intensity

$$\langle I(\vec{r})\rangle = \frac{1}{4\pi} \int I(\vec{r},\vec{\Omega})d\Omega \tag{24}$$

The average intensity does not, in general, represent the power flow but is proportional to the radiant energy at a spatial mesh point r. In equation (24) and in the remainder of this work, $I(\vec{r},\vec{\Omega})$ is the diffuse radiance at a two-dimensional spatial mesh point specified by the radius vector r. The direct (reduced) beam intensity is omitted.

In order to investigate the relative importance of multiple-scattering corrections to the Beer-Lambert law, we introduce a correction factor C which is entirely due to multiple scattering. As the target reflects isotropically, the reduced (unscattered) light intensity at a distance from the target is

$$I_r = \frac{P_o e^{-\tau}}{4\pi\ell^2} \tag{25}$$

where P_o is the power emitted by the target and $\tau = \sigma\ell$ the optical depth between the target and a receiver. The total intensity, a sum of the reduced and diffuse parts,

$$I = I_r + I_d \tag{26}$$

may be written in terms of a correction factor C to Beer-Lambert's law as

$$I = \frac{P_o e^{-\tau}}{4\pi\ell^2}(1 + C) \quad , \text{ so that } I_d = C\,\frac{P_o}{4\pi\ell^2}\,e^{-\tau} \tag{27}$$

Solving equation (27) for C, we obtain explicitly

$$C = \frac{I_d}{P_o/(4\pi\ell^2)}\,e^{\tau} \tag{28}$$

As the diffuse intensity is created within the medium due to multiple scattering, the correction factor vanishes when only target reflection and absorption are considered.

6. NUMERICAL RESULTS

The quantities of interest introduced in section 4, namely the average intensity, scattered radiance and the B/L correction factor will now be computed in x-y and r-z geometries.

6.1 Rectangular Geometry.

Figure A-2 shows the average intensity distribution for multiply-scattered laser radiation corresponding to the visual range V = 1.52 km. In figure A-3, the same result is shown with the spatial scale distorted. This displays detailed intensity variations. The distortion represents every (nonequidistant) spatial fine mesh, as defined in figure 1 and section 4, as if it were equally spaced. This feature causes the intensity peaks created by the aerosol environment and the target to be broadened and more easily recognizable in figure A-3.

In figures A-4 and A-5, the average intensity distribution is shown for a situation corresponding to V = 0.76 km where the aerosol concentration is increased to 100,000 particles per cm^3. The bimodal distribution in figures A-2 and A-3, with the target radiation being the dominant feature, becomes now a monomodal and the target is no longer easily recognizable. This result shows that for sufficiently high aerosol concentration the dominant scattered signal corresponds essentially to the interaction of laser radiation with the aerosol environment.

Dropping thus the case of higher aerosol concentration, we list in tables B-1 and B-2 (appendix B) the B/L correction factor for V = 1.52 km assuming a detector moving in a plane parallel to the surface of the earth and pointing toward the target. In actual computations the reduced intensity, as defined by equation (5), was obtained by executing our computer code in the case involving no scattering, i.e., setting the scattering coefficient of aerosols $\sigma_s = 0$. The coordinates of the detector were determined by finding a ray, in the set of discrete directions, which emanates from the target to cross the line along which the detector is assumed to move.

The use of the delta M method reduces significantly the computer time required to obtain the radiance distribution function and the correction factors. When executing the TWOTRAN code with the P_5 expansion [L= 5 in equation (8)], the CPU time was 90 sec for 1764 spatial meshes and 144 directions. Employing the delta 4 approximation results in the reduction of CPU time down to 45 sec. The two columns of the correction factors in tables B-1 and B-2 refer to these two ways of computation.

6.2 Cylindrical Geometry.

Leaving unchanged other parameters, we proceed to the cylindrical (r-z) geometry model. Figures A-6 and A-7 show the average intensity when the visual range is 1.52 km, while figures A-8 and A-9 correspond to the visual range of 0.76 km. As before, the target signal becomes undistinguishable from the aerosol-scattered radiation as the visual range becomes smaller than the distance between laser source and target. Tables B-3 and B-4 list the scattered radiance and the B/L correction factors for the aerosol model with visual range V = 1.52 km in the case of a detector moving along a line parallel to the beam axis.

7. DISCUSSION

Comparing the results contained in the figures A-2 to A-5 (x-y model) with those of figures A-6 to A-9 (r-z model), we find the same characteristic features in the diffuse average intensity. In particular, the scattered radiance from the target becomes negligibly small as the visual range is shorter than the distance between the source and the target. We thus conclude that the x-y and r-z geometry models are qualitatively equivalent as far as the target detection is concerned. The infinite z direction in x-y geometry is only an expression of a symmetry condition and is not a perturbing factor as long as results are considered only in the x-y plane.

To the extent that the plots of average intensity show a qualitative agreement between the two geometries, insight into the quantitative results can be gained by inspecting tables B-1 through B-4. For smaller optical depths, up to about $\tau = 1.0$, the agreement in the calculated correction factors is indeed quite satisfactory and suggests a functional form of the correction factor described by a universal function of only. As the distance between the target and the detector increases, the observed discrepancies can be attributed to the ray effect. This phenomenon, due to the basic discrete ordinate approximation itself, consists, in essence, in solving the transport equation along a limited number of discrete characteristics (i.e., rays). For the sake of illustration, let us consider an isotropic line source in a purely absorbing medium. Then, clearly, the resultant analytical radiance distribution function will possess azimuthal symmetry about the source line. But if we apply the discrete ordinates method to this situation, the resultant radiance will consist of a stepfunction in the azimuthal angle because only specific directions emanating from the line source will contain the source photons. Thus the discrete ordinates method approximates the azimuthally uniform radiance by a discrete set of values at discrete azimuthal angles. The existing remedies like those transforming the discrete ordinates equations to spherical-harmonic form,[18-20] will be an object of future research.

In summary, we have applied the discrete ordinates code TWOTRAN to the problem of laser beam propagation and multiple scattering in dense aerosols. The delta M approximation has proven to be of definite advantage for our applications. The main result of our investigation consists in validating the use of an x-y geometry model in describing a realistic three-dimensional scenario. This is achieved by computing the average intensity and B/L correction factor in x-y and r-z geometries. The effect of aerosol concentration on the detectability of a target follows independently of the choice of x-y or r-z geometry. In addition, as we have shown by evaluating the multiple-scattering corrections to the Beer-Lambert law, the multiple-scattering contribution to the target signature can be quite dramatic even for a moderate optical thickness of the order of 2. As the optical thickness increases beyond $\tau = 1.5$, the correction factor grows very rapidly. The problem, however, in the context of the discussed scenario becomes less realistic due to the decreased visual range.

Of definite interest would be a further study of the ray effect as well as a comparison of the results obtained with the results employing the small angle[21-23] and diffusion approximations.[24]

LITERATURE CITED

1. Chandrasekhar, S. Radiative Transfer. Dover, New York. 1960.

2. Duderstadt, J. J. and Martin, W. R. Transport Theory. John Wiley & Sons, New York, New York. 1979 p 420.

3. Liou, K. N. A Numerical Experiment in Chandrasekhar's Discrete-Ordinate Method for Radiative Transfer: Applications to Cloudy and Hazy Atmospheres. J. Atmos. Sci. 30, 1303 (1973).

4. Liou, K. N. An Introduction to Atmospheric Radiation. Academic Press, New York, New York, 1980.

5. Lenoble, J. Editor. Standard Procedures to Compute Atmospheric Radiative Transfer in a Scattering Atmosphere, Radiation Commission, IAMAP. National Center for Atmospheric Research. Boulder, Colorado. 1977.

6. Bell, G. I. and Glasstone, S. Nuclear Reactor Theory. Van Nostrand Reinhold Company, New York, New York. 1970.

7. Gerstl, S. A. W. Application of Modern Neutron Transport Methods to Atmospheric Radiative Transfer. Los Alamos Scientific Laboratory Report LA-UR-80-1403; also Int. Radiation Symposium. Fort Collins, Colorado. August 11-16, 1980, Vol. of Extended Abstracts, pp. 500-502 (1980).

8. Lathrop, K. D. THREETRAN: A Program to Solve the Multigroup Discrete Ordinates Transport Equation in (x,y,z) Geometry. Los Alamos Scientific Laboratory Report LA-6333-MS. May 1976.

9. Fowler, B. W. Technical Report C-78-3. An Investigation of Radiation Transfer Through Aerosols. US. Army Missile Research and Development Command. June 1978. UNCLASSIFIED Report.

10. Fowler, B. W. and Sung, C. C. Radiative Transfer in Two Dimensions Through Fog. Appl. Opt. 17, 1797 (1978).

11. Lathrop, K. D. and Brinkley, F. W. TWOTRAN-II: An Interfaced Exportable Version of the TWOTRAN Code for Two-Dimensional Transport. Los Alamos Scientific Laboratory Report LA-4848-MS. July 1973.

12. Wiscombe, W. J. The Delta-M Method: Rapid Yet Accurate Radiativen Flux Calculations for Strongly Asymmetric Phase Functions. J. Atmos. Sci. 34, 1408 (1977).

13. Joseph, J. H, Wiscombe, W. J., and Weinman, J. A. The Delta-Eddington Approximation for Radiative Flux Transfer. J. Atmos Sci. 33, 2452 (1976).

14. McKellar, Bruce H. J., and Box, Michael A. The Scaling Group of the Radiative Transfer Equation. J. Atmos. Sci. 38, 1063 (1981).

15. Shettle, E. P. and Fenn, R. W. Air Force Geophysics Laboratory Report AFGL-TR-79-0214. Models of the Aerosols of the Lower Atmosphere and the Effects of Humidity Variations on Their Optical Properties. September 1979. UNCLASSIFIED Report.

16. Shirkey, R. C., Miller, A., Goedecke, G. H. and Behl, Y. K. Atmospheric Sciences Laboratory Report ARCSL-TR-0062. Single Scattering Code AGAUSX: Theory Applications, Comparisons, and Listing. July 1980. UNCLASSIFIED Report.

17. Burlbaw, E. and Miller, A. ASL-CR-81-0780-1. Atmospheric Sciences Laboratory Report. Modification of Single Scattering Model AGAUS. May 1981. UNCLASSIFIED Report.

18. Jung, J. Jungchang, Chijiwa, Hiroshii, Kobajashi, Keisuki, and Nishikara, Hiroshi. Discrete Ordinate Neutron Transport to PL Approximation. Nucl. Sci. Eng 49, (1) (1972).

19. Lathrop, K. D. Rate Effects in Discrete Ordinates Equations. Nucl. Sci Eng. 32, 357 (1968).

20. Lathrop, K. D. Remedies for Ray Effects. Nucl. Sci. Eng. 45, 255 (1971).

21. Fante, R. L. Electromagnetic Beam Propagation in Turbulent Media - An Update. Proc. IEEE 68, 1424 (1980).

22. Tam, W. G. and Zardecki, A. Multiple-Scattering of a Laser Beam by Radiational and Advective Fogs. Opt. Acta. 26, 659 (1972).

23. Deepak, Adarsh, Farrukh, Usamah O., and Zardecki, Andrew. Significance of Higher-Order Multiple Scattering for Laser Beam Propagation Through Hazes, Fogs and Clouds. Appl. Opt. 21, 439 (1981).

24. Tam, W. G. and Zardecki, Andrew. Off-Axis Propagation of a Laser Beam in Low-Visibility Weather Conditions. Appl. Opt. 19, 2822 (1980).

APPENDIX A

FIGURES

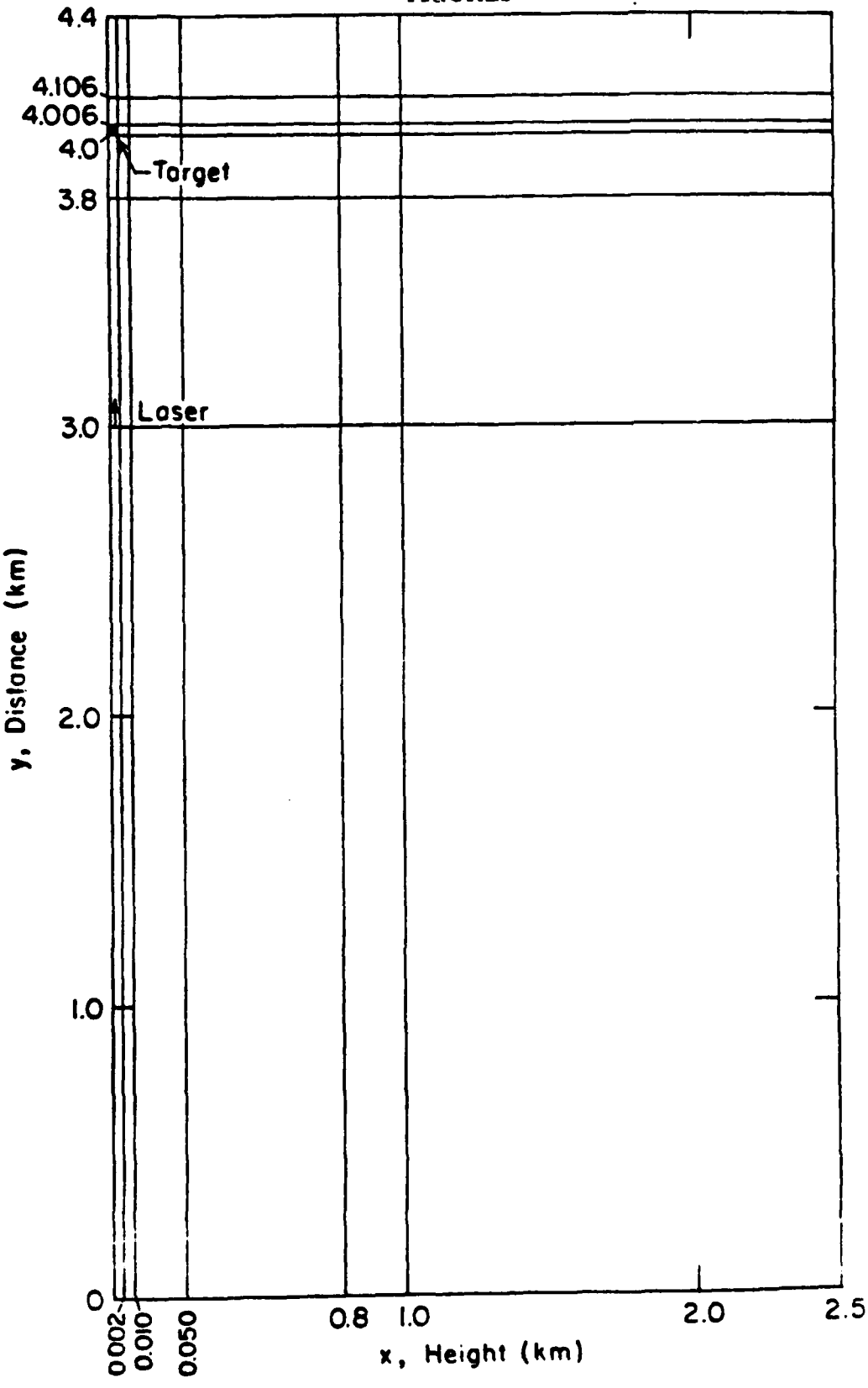

Figure A-1. Locations of the Laser Source and the Isotropically Scattering Target in the x-y (r-z) Plane. The lines indicate the coarse mesh boundaries as required by the TWOTRAN code.

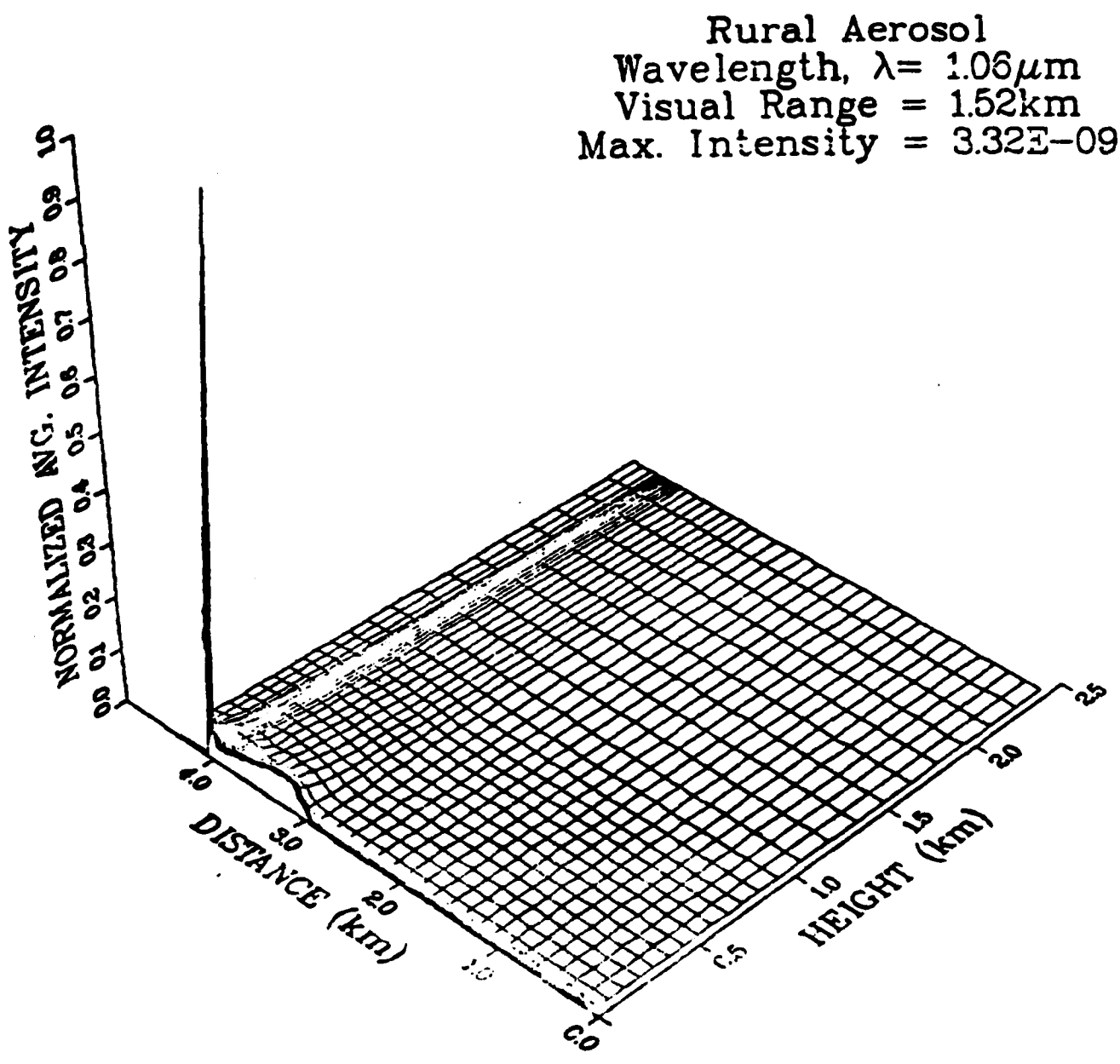

Figure A-2. Normalized Average Intensity on a Real Scale Lattice of Partial Mesh Points in x-y Geometry. Visual Range 1.52 km.

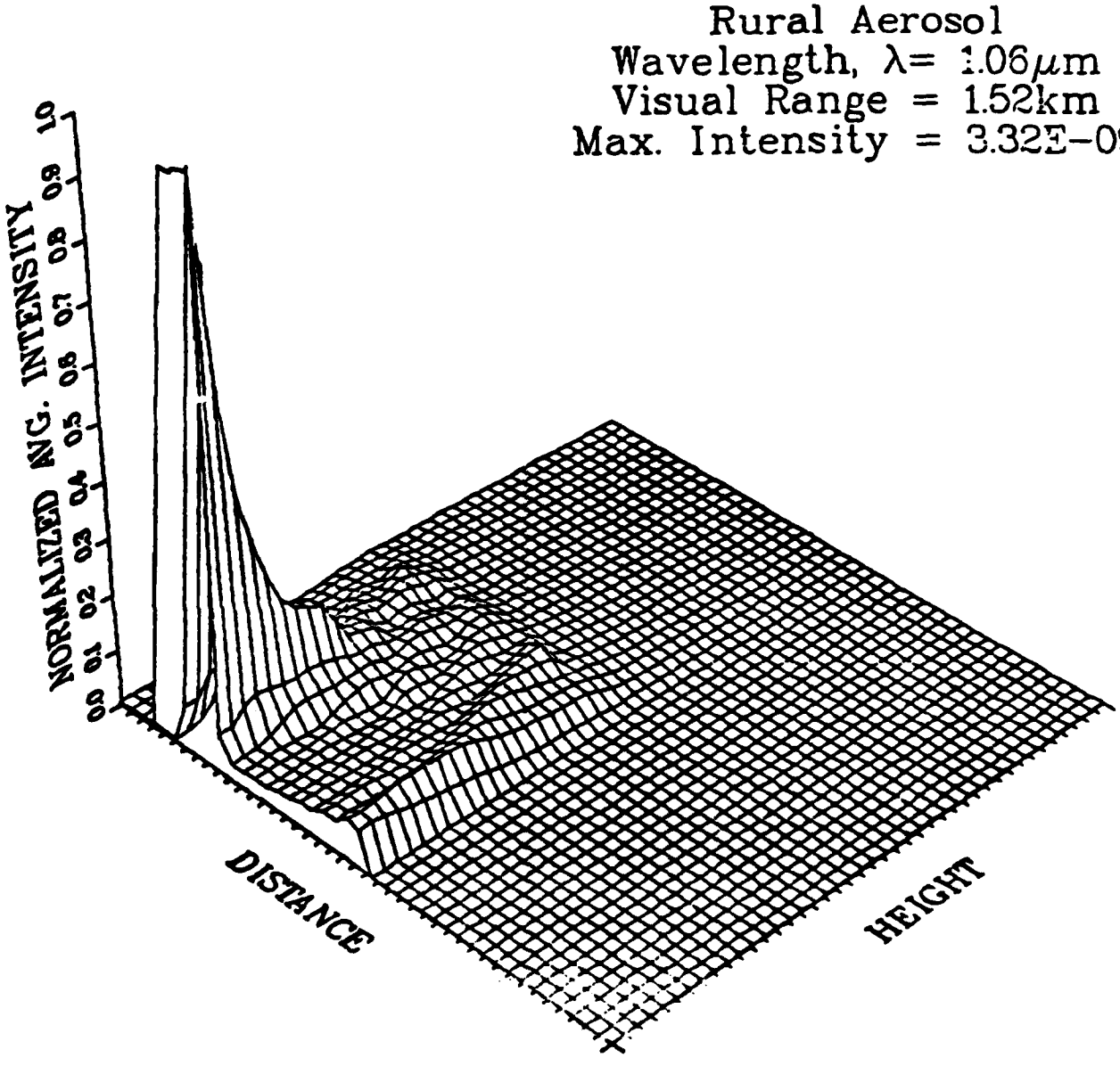

Figure A-3. Normalized Average Intensity on a Distorted Lattice of Spatial Mesh Points in x-y Geometry. Visual Range 1.52 km.

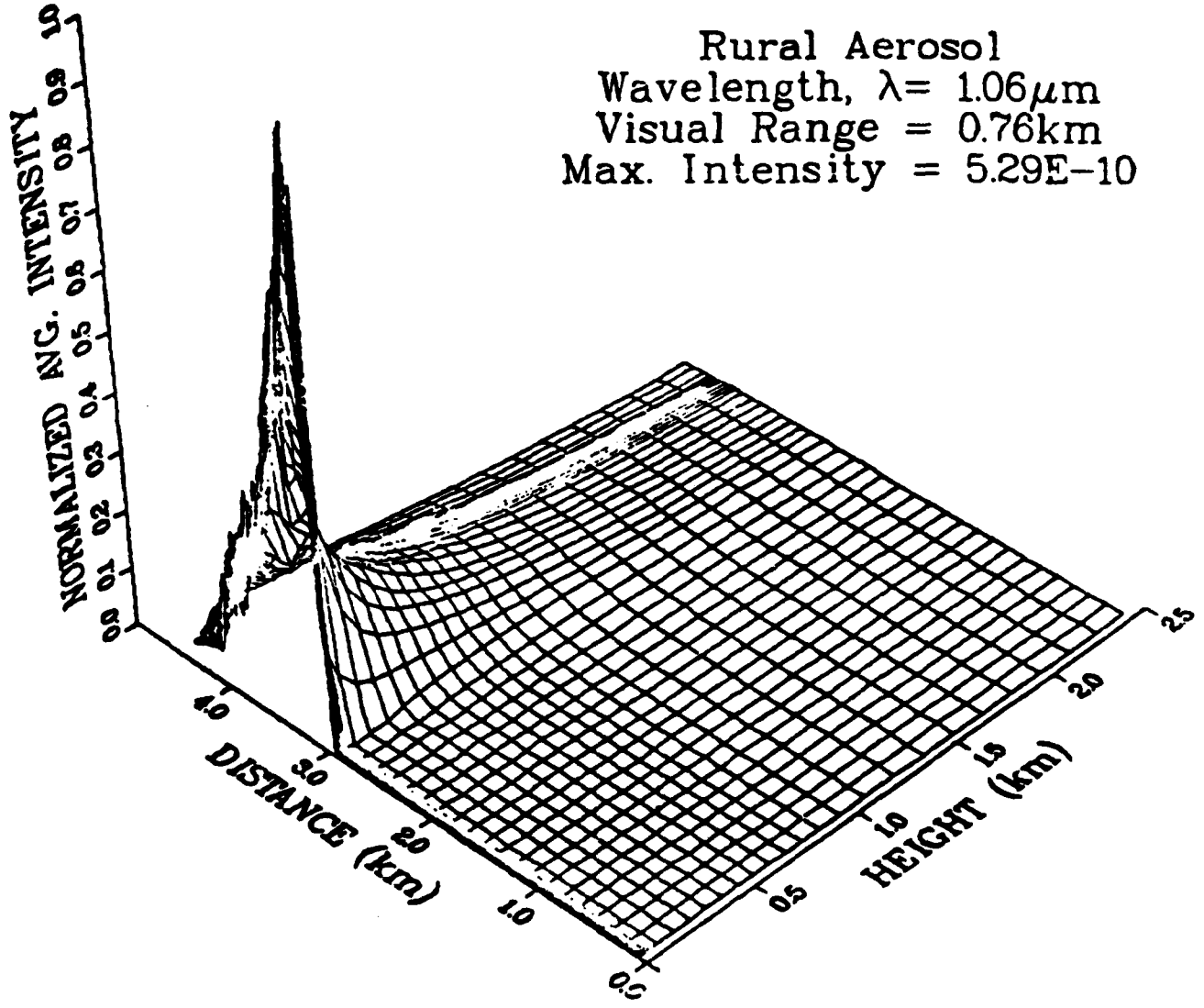

Figure A-4. Normalized Average Intensity on a Real Scale Lattice of Spatial Mesh Points in x-y Geometry. Visual Range 0.76 km.

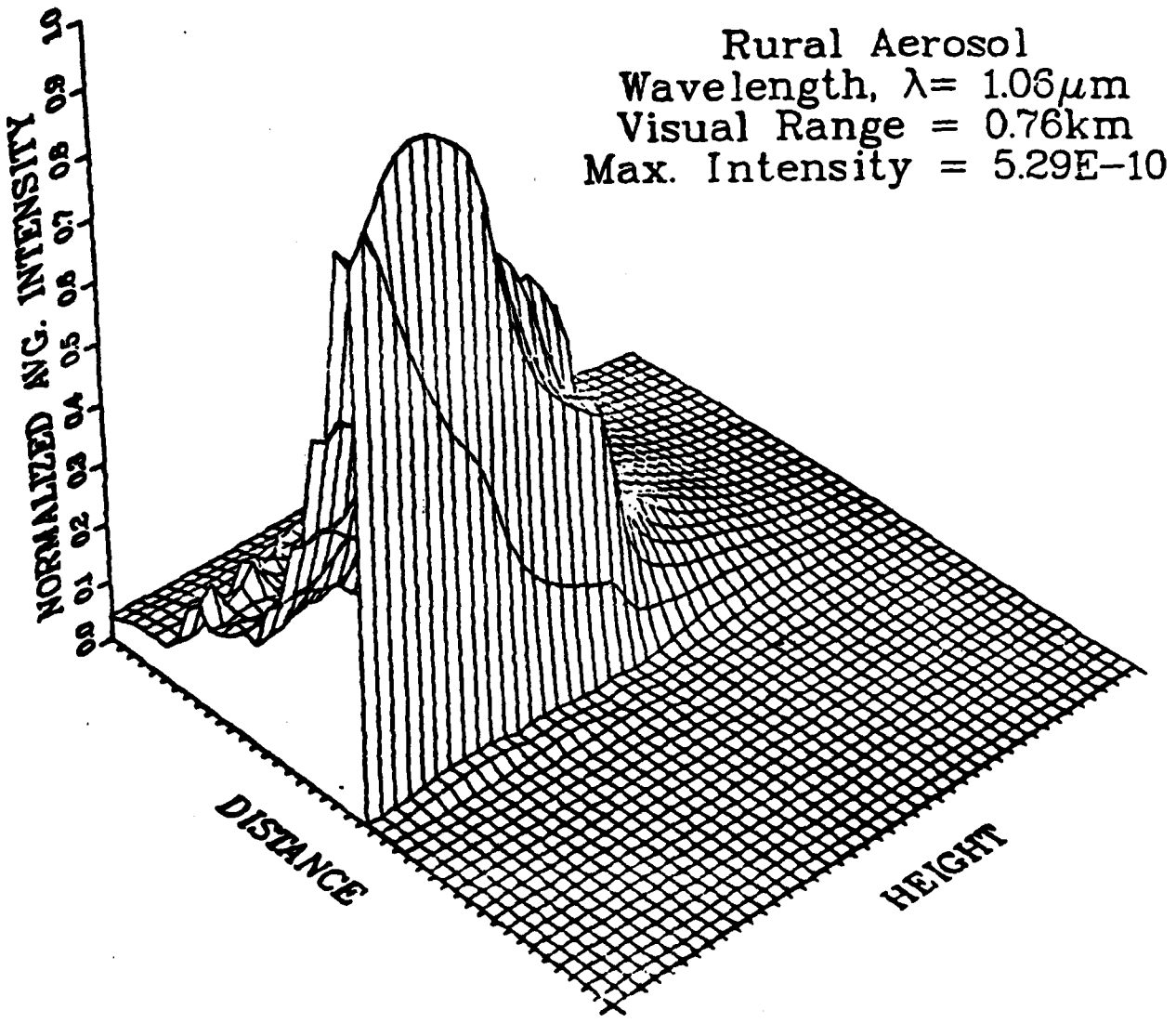

Figure A-5. Normalized Average Intensity on a Distorted Lattice of Spatial Mesh Points in x-y Geometry. Visual Range 0.76 km.

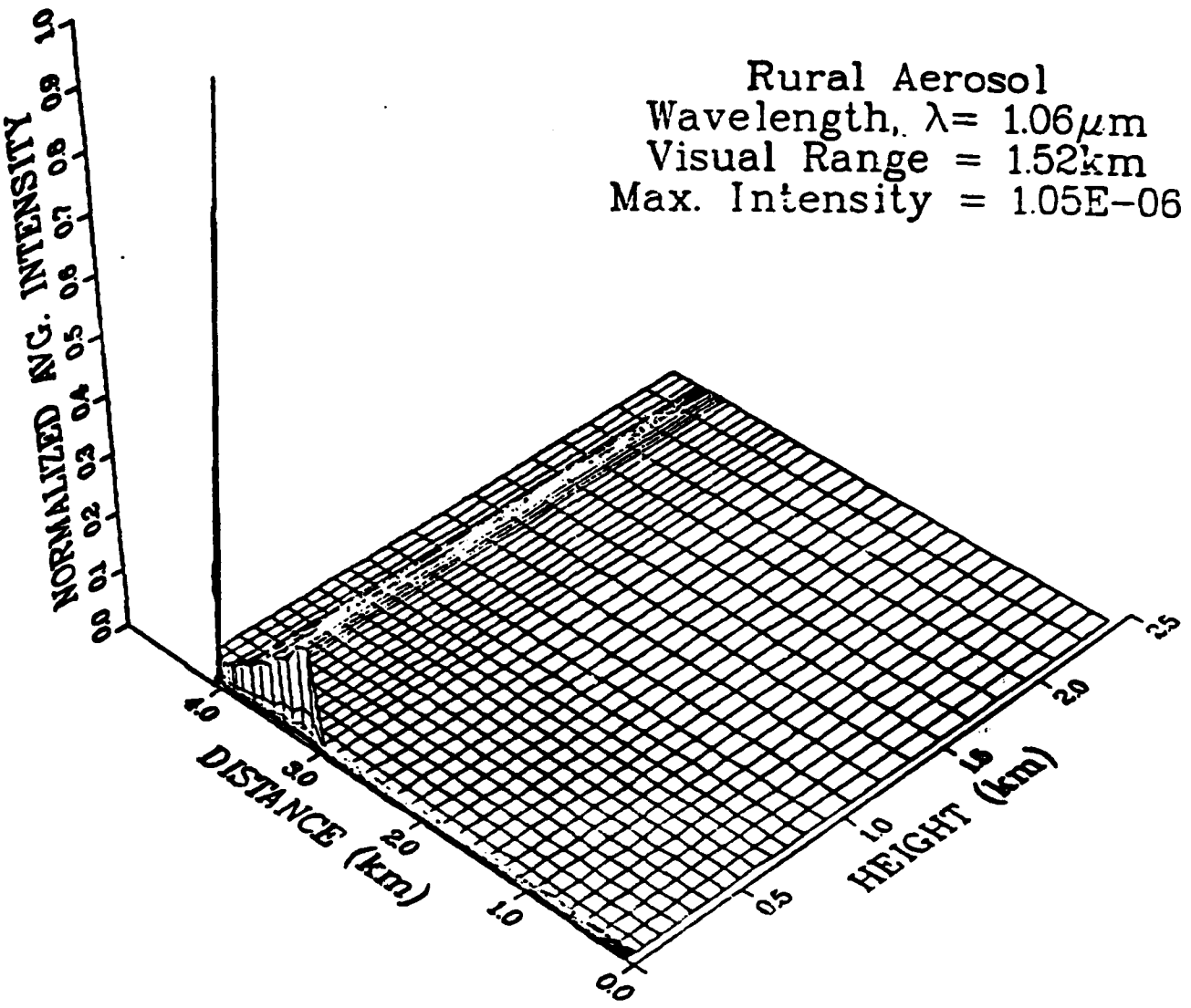

Figure A-6. Normalized Average Intensity on a Real Scale Lattice of Spatial Mesh Points in r–z Geometry. Visual Range 1.52 km.

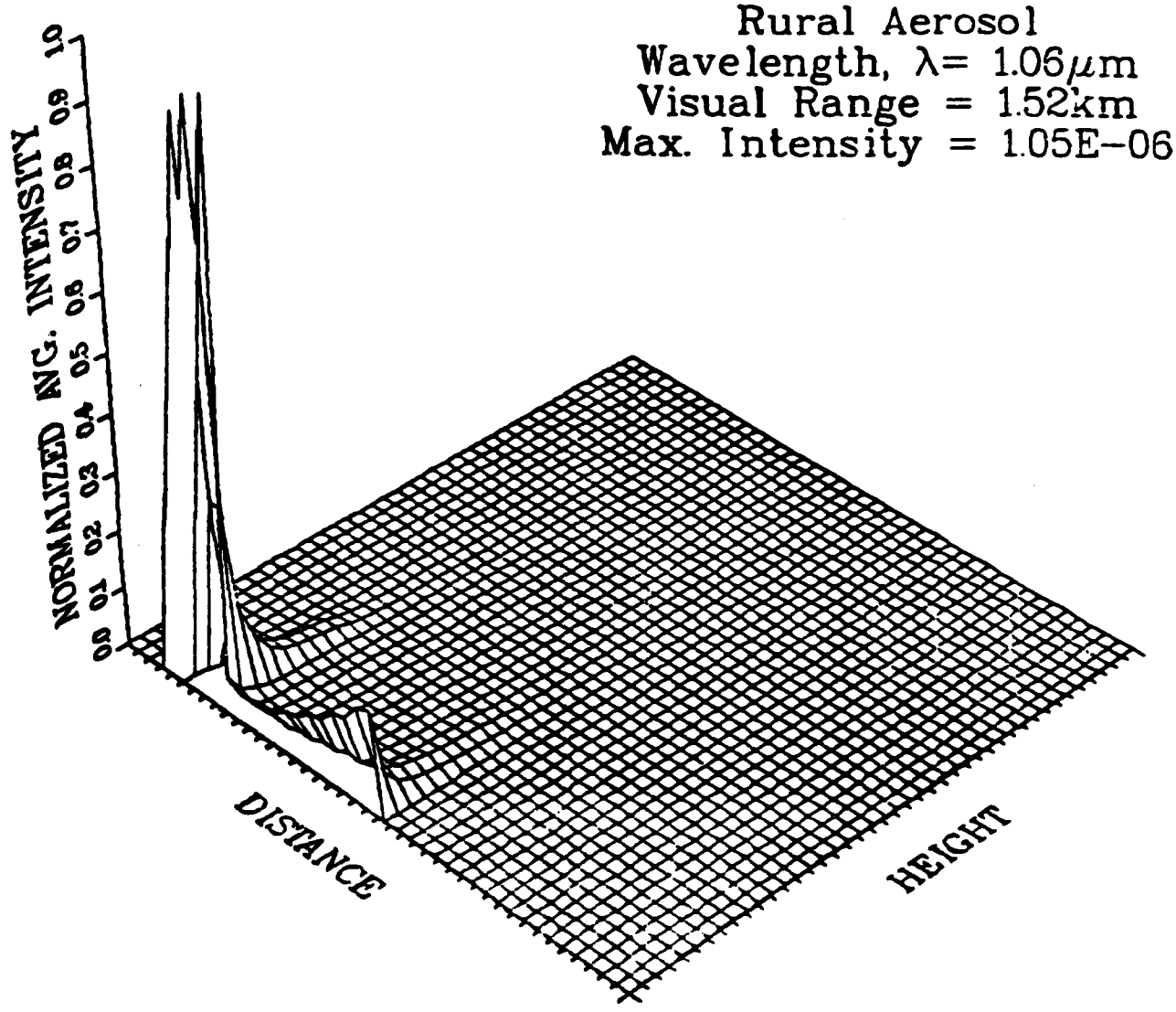

Figure A-7. Normalized Average Intensity on a Distorted Lattice of Spatial Mesh Points in r-z Geometry. Visual Range 1.52 km.

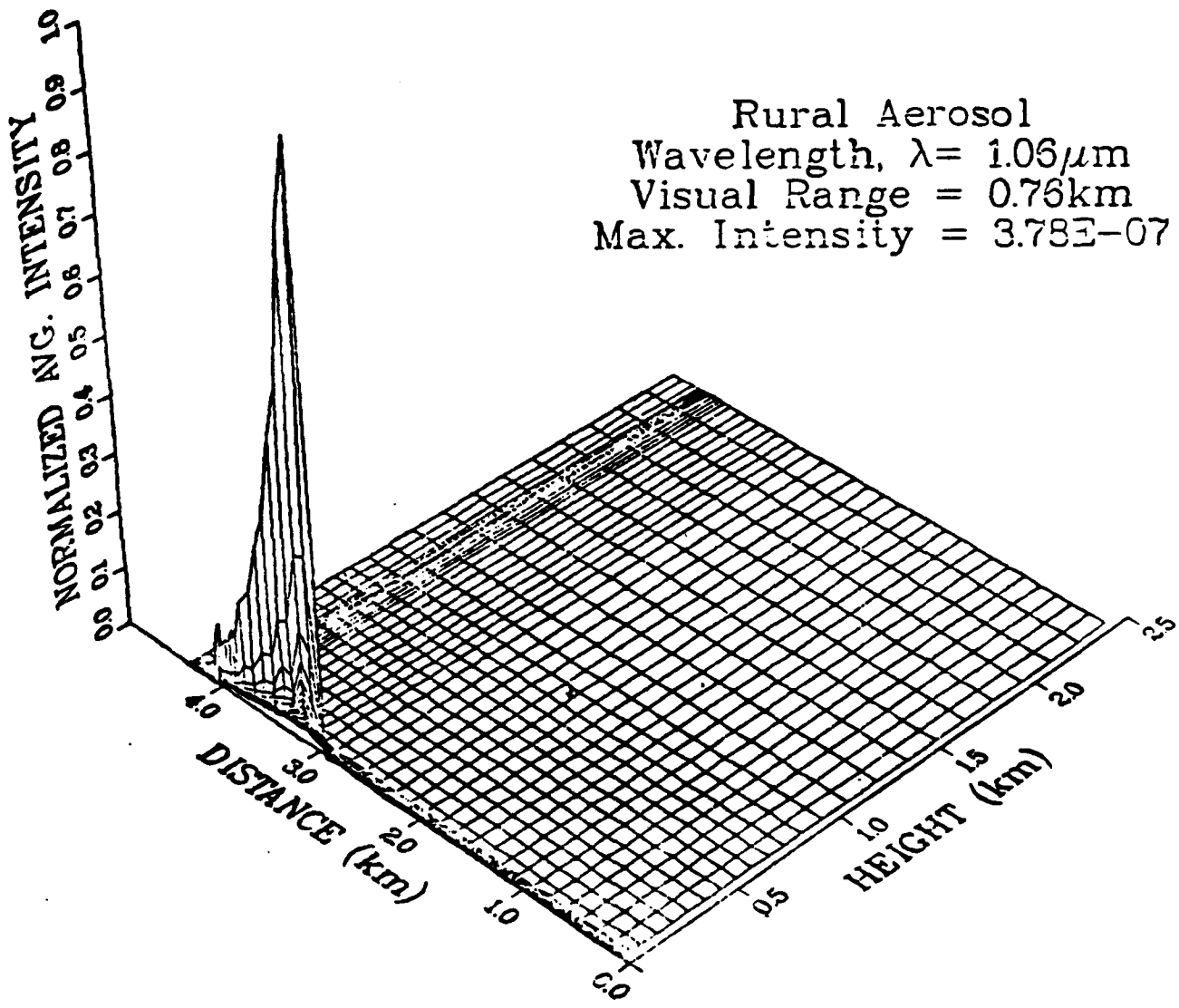

Figure A-8. Normalized Average Intensity on a Real Scale Lattice of Spatial Mesh Points in r-z Geometry. Visual Range 0.76 km.

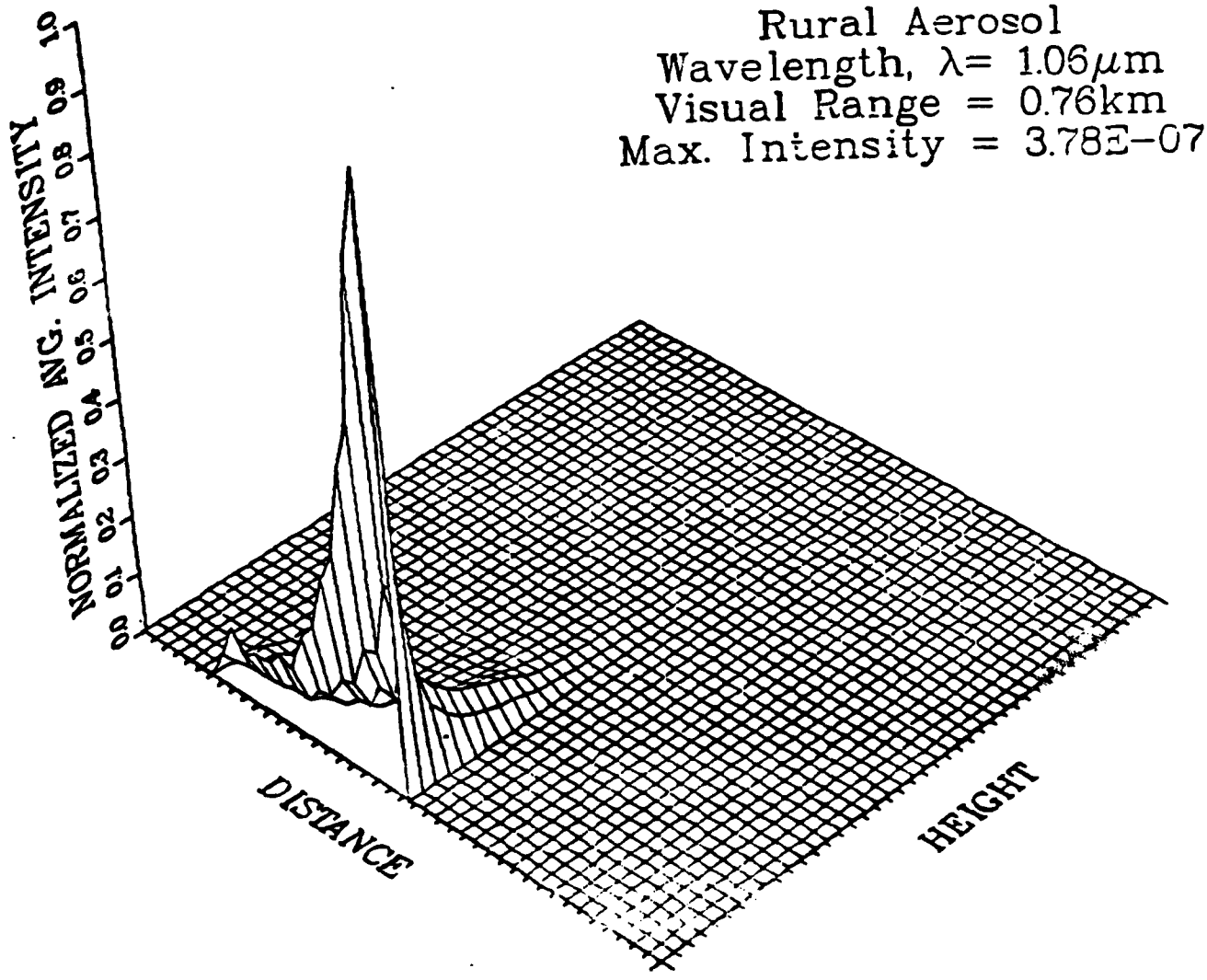

Figure A-9. Normalized Average Intensity on a Distorted Lattice of Spatial Mesh Points in r-z Geometry. Visual Range 0.76 km.

Blank

APPENDIX B

TABLES

Table B-1. X-Y Geometry: Target Coordinates x = 0.001 km, y = 4.000 km: Detector Height = 0.200 km

Detector's y coordinate	Optical depth	Radiance	Beer/Lambert correction factor	
			P5	Delta -4
km		$w.m^{-2}.sr^{-1}$		
2.515	1.978	2.9792×10^{-1}	1.14	1.46
3.529	0.675	1.3051×10^{-1}	0.37	0.43
3.767	0.406	1.8615×10^{-1}	0.29	0.29
3.822	0.353	3.0306×10^{-1}	0.21	0.21
3.867	0.317	3.8526×10^{-1}	0.15	0.15

Table B-2. X-Y Geometry: Target Coordinates x = 0.001 km, y = 4.000 km: Detector Height = 0.500 km

Detector's y coordinate	Optical depth	Radiance	Beer/Lambert correction factor	
			P5	Delta -4
km		$w.m^{-2}.sr^{-1}$		
2.824	1.687	2.9857×10^{-2}	1.44	1.72
3.556	0.883	1.1178×10^{-1}	0.74	0.77
3.668	0.792	1.0735×10^{-1}	0.64	0.66
3.904	0.672	1.9973×10^{-1}	0.32	0.38

Table B-3. R-Z Geometry: Target Coordinates r = 0.0 km, z = 4.000 km: Detector Height r = 0.200 km

Detector's y coordinate	Optical depth	Radiance	Beer/Lambert correction factor	
			P5	Delta -4
km		$w.m^{-2}.sr^{-1}$		
2.959	1.398	8.9695×10^{-2}	0.64	0.83
3.699	0.477	5.1730×10^{-1}	0.38	0.41
3.775	0.397	9.4538×10^{-1}	0.27	0.28
3.829	0.348	$2.8858 \times 10^{+0}$	0.13	0.14

Table B-4. R-Z Geometry: Target Coordinates r = 0.0 km, z = 4.000 km: Detector Height r = 0.500 km.

Detector's y coordinate	Optical depth	Radiance	Beer/Lambert correction factor	
			P5	Delta -4
km		$w.m^{-2}.sr^{-1}$		
1.398	3.496	2.6520×10^{-3}	1.66	2.78
2.898	1.596	3.8658×10^{-2}	0.85	1.92
3.247	1.193	2.5389×10^{-1}	0.69	0.82
3.437	0.993	2.2313×10^{-1}	0.55	0.65
3.571	0.869	1.6951×10^{-1}	0.50	0.61
3.682	0.782	2.2435×10^{-1}	0.36	0.44
3.787	0.717	2.2986×10^{-1}	0.35	0.41

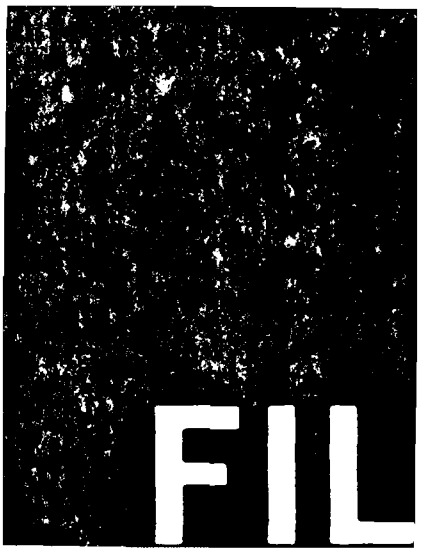
FIL